Data Descriptor

Not peer-reviewed version

Whole-Rock Geochemical Dataset of Late Variscan Intrusive Rocks from the Serre Batholith (Calabria, Southern Italy)

Annamaria Fornelli , Francesca Micheletti , Fabrizio Tursi , Vincenzo Festa *

Posted Date: 2 May 2026

doi: 10.20944/preprints202604.2200.v1

Keywords: geochemistry; granitoids; Serre Massif

Data Descriptor

Whole-Rock Geochemical Dataset of Late Variscan Intrusive Rocks from the Serre Batholith (Calabria, Southern Italy)

Annamaria Fornelli [1], Francesca Micheletti [1], Fabrizio Tursi [2] and Vincenzo Festa [1,*]

[1] Dipartimento di Scienze della Terra e Geoambientali, Università degli Studi di Bari Aldo Moro, 70125 Bari, Italy

[2] Dipartimento di Scienze della Terra, Università degli Studi di Torino, 10125 Torino, Italy

* Correspondence: vincenzo.festa@uniba.it

Abstract

We present a new whole-rock geochemical dataset for intrusive rocks of the late Variscan Serre batholith (Calabria, southern Italy), a well-exposed section of tilted continental crust emplaced between ~305 and 292 Ma. The dataset includes major, trace and rare earth element (REE) analyses for 74 samples collected from the main plutonic units, ranging from tonalites and quartz-diorites at deeper structural levels to peraluminous granites at shallower levels, as well as leucosomes from associated migmatitic metasediments. Analytical data were obtained using X-ray fluorescence (XRF) and inductively coupled plasma mass spectrometry (ICP-MS). The dataset integrates new and previously published geochemical data into a consistent and reusable format, including sample locations (WGS84), lithological classification and stratigraphic attribution. Sampling sites are also provided as a downloadable geospatial (.kmz) file for visualization in GIS platforms. The dataset is made available as a supplementary Excel file. These data are intended to support a wide range of applications, including petrogenetic studies of granitoid magmatism and investigations of water–rock interaction processes in crystalline aquifers. The dataset represents a valuable resource for both fundamental and applied geoscientific research.

Dataset: supplement to this paper

Dataset License: Creative Commons Attributions CC-BY-NC-ND license

Keywords: geochemistry; granitoids; Serre Massif

---

1. Summary

Whole-rock chemical data for plutonic rocks, including major, minor, and trace elements, are fundamental for constraining the origin of intrusive magmas and the geodynamic context of their generation and emplacement (e.g., [1]). In this regard, the Serre Carboniferous-early Permian composite batholith [2], exposed in in the Serre Massif of central Calabria (southern Italy; Figure 1a), has been of great interest to magmatic petrologists since the 1970s, as evidenced by the extensive geochemical data reported in numerous research papers [3–24].

 doi:10.20944/preprints202604.2200.v1

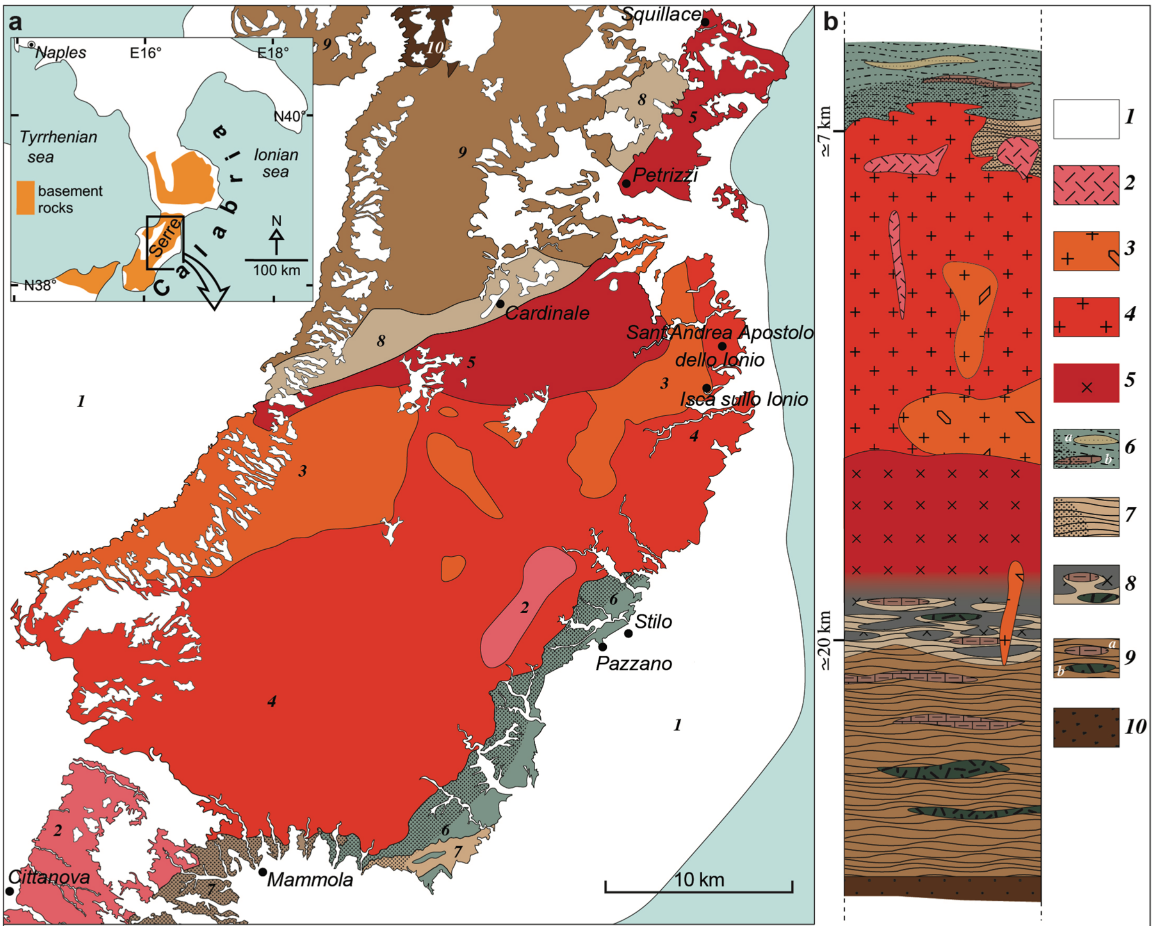

1. Sedimentary cover (*Mesozoic - Cenozoic*). Serre batholith's plutonic units, i.e., intermediate late-Variscan continental crust (*Upper Pennsylnanian - late Cisuralian*): **2.** fine-grained strongly peraluminous granites - *Cittanova* unit; **3.** granites and granodiorites with K-feldspar megacrysts - *Isca sullo Ionio* unit; **4.** medium-grained granodiorites, granites and monzogranites - *Sant'Andrea Apostolo dello Ionio/Serre* unit; **5.** Tonalites and quartz-diorites - *Squillace-Petrizzi* and *Cardinale* units. Late-Variscan upper continental crust: **6.** Slates, phyllites with interbedded (a) marbles and (b) metavolcanites of the Stilo-Pazzano tectono-metamorphic unit (*Cambrian - Carboniferous* protoliths)–dots indicate the metamorphic contact aureole due to the Serre batholith; **7.** Micaschists and paragneisses of the Mammola tectono-metamorphic unit (*Precambrian* protoliths)–dots indicate the metamorphic contact aureole due to the Serre batholith. Late-Variscan lower continental crust: **8.** Migmatitic border zone due to the Serre batholith. **9.** Migmatitic paragneisses with interbedded (a) marbles and (b) metabasites (*Precambrian* protoliths). **10.** Felsic granulites (*Precambrian* protoliths).

Figure 1. (**a**) Geological sketch-map of the Serre Massif; legend as in Figure 1b (modified after [29,30,32–36]). (**b**) Schematic stratigraphic column of the late-Variscan continental crust exposed in the Serre Massif; paleodepths are indicated on the left (modified after [26,36]).

The present study presents a publicly available chemical dataset of intrusive rocks from the composite Serre batholith. This dataset is intended for use in fundamental research on magma evolution as well as applied geological investigations, such as the interaction between plutonic rock bodies and their hosted groundwater systems (e.g., [25]).

Within the tilted late Variscan continental crustal block exposed in the Serre Massif (e.g., [26,27]), nearly tabular rock granitoids bodies constitute the Serre batholith, which occupies the intermediate crustal level [28]. The emplacement and construction of this plutonic stack occurred between approximately 305 and 292 Ma (e.g., [21,29]) at depths ranging from roughly 20 to 7 km [28], between the lower and upper continental crust (Figure 1b). Overall, the stratigraphy of the Serre batholith is geometrically characterized, from the bottom (in the northern area), upward (in the southern portion), by plutonic bodies dominated by: tonalites and quartz-diorites (i.e., *Squillace-Petrizzi* and *Cardinale* units–5 in Figure 1a,b), coarse- to medium-grained granodiorites, granites, and monzogranites (i.e., *Sant'Andrea Apostolo dello Ionio/Serre* unit–4 in Figure 1a,b), granites and granodiorites with K-feldspar megacrysts (i.e., *Isca sullo Ionio* unit–3 in Figure 1a,b); and fine-grained, strongly peraluminous granites (i.e., *Cittanova* unit–2 in Figure 1a,b) (Figure 1a,b) [30,31]. These main plutonic units were subsequently intruded by porphyritic dikes during the late Permian [18].

 doi:10.20944/preprints202604.2200.v1

At the base of the batholith, a migmatitic border zone (migmatitic unit 8 in Figure 1a,b) developed within high-grade metasedimentary host rocks [9]. During regional metamorphism, these metasediments-predominantely metapelites, metarenites, and metagreywakes underwent granulite-facies conditions and partial melting (migmatitic paragneisses metamorphic unit 9 in Figure 1a,b) [16]. The resulting melts were removed from the source rocks, contributing to the growth of the Serre batholith, while the remaining fractions were trapped within the metasediments to forme leucosomes. Notably, these leucosomes do not represent the exact in-situ complements to the adjacent melanosomes [15,32]. At the roof of the batholith, magmas intruded phyllites and greenschists- to amphibolite-facies paragneisses; here, contact metamorphism produced a broad aureole characterized by the growth of biotite, andalusite, and cordierite (metamorphic units 6 and 7 in Figure 1a,b) (e.g., [33,34]).

2. Data Description

A total of 74 samples were collected from the various intrusive bodies of the exposed Serre batholith, as well as from leucosomes within the high-grade metasediments. The WGS84 geographic coordinates for each sample, along with their predominant lithotype and the related lithostratigraphic unit (as in Figure 1a,b), are provided in Table 1. Sampling locations can be also displayed in Google Earth opening the file as in Geographic Data S1, i.e., *Samples_Serre.kmz*.

Table 1. Granitoid samples from the Serre Massif.

Sample	Main lithological features	Metamorphic (m.) or plutonic (p.) unit	Longitude	Latitude
LFC1A	migmatite leucosome concordant with metapelite host	migmatitic paragneisses m. unit	16°17′56.09″E	38°50′43.91″N
LFC5	migmatite leucosome concordant with metapelite host	migmatitic paragneisses m. unit	16°18′20.83″E	38°48′15.56″N
LFC7	migmatite leucosome concordant with metapelite host	migmatitic paragneisses m. unit	16°17′22.13″E	38°43′18.11″N
KIS15	migmatite leucosome concordant with metapelite host	migmatitic paragneisses m. unit	16° 5′4.91″E	38°41′23.13″N
Kis 8a	migmatite leucosome concordant with metapelite host	migmatitic paragneisses m. unit	16°23′43″E	38°46′15″N
Kis 11a	migmatite leucosome concordant with metapelite host	migmatitic paragneisses m. unit	16°27′35.00″E	38°50′31.00″N
Kis16	migmatite leucosome concordant with metapelite host	migmatitic paragneisses m. unit	16° 5′21.83″E	38°41′29.54″N
LFC8	migmatite leucosome concordant with metapelite host	migmatitic paragneisses m. unit	16°27′35.00″E	38°50′31.00″N
MFS9	migmatite leucosome concordant with metapelite host	migmatitic paragneisses m. unit	16°17′41.58″E	38°43′22.87″N
MFS10	migmatite leucosome concordant with metapelite host	migmatitic paragneisses m. unit	16°17′30.85″E	38°42′53.88″N

 doi:10.20944/preprints202604.2200.v1

MFS11	migmatite leucosome concordant with metapelite host	migmatitic paragneisses m. unit	16°17′32.98″E	38°41′14.08″N
MFS12	migmatite leucosome concordant with metapelite host	migmatitic paragneisses m. unit	16°17′32.98″E	38°41′14.08″N
MFS13	migmatite leucosome concordant with metapelite host	migmatitic paragneisses m. unit	16°22′49.09″E	38°42′52.76″N
LFC13I	migmatite leucosome concordant with metagreywake host	migmatitic paragneisses m. unit	16°17′45.74″E	38°50′41.09″N
LFC12	migmatite leucosome concordant with metagreywake host	migmatitic paragneisses m. unit	16°17′45.62″E	38°50′42.34″N
KIS18	migmatite leucosome discordant with metapelite host	migmatitic paragneisses m. unit	16° 5′52.00″E	38°41′25.00″N
Kis17	migmatite leucosome discordant with metapelite host	migmatitic paragneisses m. unit	16° 5′21.83″E	38°41′29.54″N
LFC4	migmatite leucosome discordant with metagreywake host	migmatitic paragneisses m. unit	16°17′56.97″E	38°50′53.58″N
LFC11B	migmatite leucosome discordant with metagreywake host	migmatitic paragneisses m. unit	16°17′56.02″E	38°50′42.34″N
LFC6	migmatite leucosome discordant with metagreywake host	migmatitic paragneisses m. unit	16°17′19.96″E	38°45′29.86″N
LFC1O	migmatite leucosome discordant with metagreywake host	migmatitic paragneisses m. unit	16°26′2.00″E	38°48′33.00″N
SCA1	biotite-amphibole bearing granitoids	Sant’Andrea Apostolo dello Ionio/Serre p. unit	16°31′0.09″E	38°33′12.38″N
SCA2	biotite-amphibole bearing granitoids	Sant’Andrea Apostolo dello Ionio/Serre p. unit	16°31′15.86″E	38°33′11.38″N
SCA3	biotite-amphibole bearing granitoids	Sant’Andrea Apostolo dello Ionio/Serre p. unit	16°30′49.4″E	38°33′19″N
SCA4	biotite-amphibole bearing granitoids	Sant’Andrea Apostolo dello Ionio/Serre p. unit	16°32′29.28″E	38°34′29.91″N
SCA5	biotite-amphibole bearing granitoids	Sant’Andrea Apostolo dello Ionio/Serre p. unit	16°30′45.47″E	38°33′14.70″N
SCA6	biotite-amphibole bearing granitoids	Sant’Andrea Apostolo dello Ionio/Serre p. unit	16°29′41.19″E	38°32′2.52″N

 doi:10.20944/preprints202604.2200.v1

SCA7	biotite-amphibole bearing granitoids	Sant'Andrea Apostolo dello Ionio/Serre p. unit	16°30′54.11″E	38°32′57.24″N
SCA8	biotite-amphibole bearing granitoids	Sant'Andrea Apostolo dello Ionio/Serre p. unit	16°30′53.51″E	38°32′6.77″N
SCA9	biotite-amphibole bearing granitoids	Sant'Andrea Apostolo dello Ionio/Serre p. unit	16°28′51.80″E	38°32′17.86″N
SCA10	biotite-amphibole bearing granitoids	Sant'Andrea Apostolo dello Ionio/Serre p. unit	16°30′47.60″E	38°32′15.80″N
SCA11	biotite-amphibole bearing granitoids	Sant'Andrea Apostolo dello Ionio/Serre p. unit	16°30′22.4″E	38°32′36″N
SCA12	biotite-amphibole bearing granitoids	Sant'Andrea Apostolo dello Ionio/Serre p. unit	16°30′29.83″E	38°32′29.16″N
SCA13	biotite-amphibole bearing granitoids	Sant'Andrea Apostolo dello Ionio/Serre p. unit	16°32′15.86″E	38°34′15.87″N
SCA14	biotite-amphibole bearing granitoids	Sant'Andrea Apostolo dello Ionio/Serre p. unit	16°31′12.27″E	38°33′38.24″N
SCA15	biotite-amphibole bearing granitoids	Sant'Andrea Apostolo dello Ionio/Serre p. unit	16°30′38.85″E	38°32′36.72″N
SCA9	biotite-muscovite bearing granitoids	Sant'Andrea Apostolo dello Ionio/Serre p. unit	16°31′34.4″E	38°34′32″N
SCA9a	biotite-muscovite bearing granitoids	Sant'Andrea Apostolo dello Ionio/Serre p. unit	16°31′34.4″E	38°34′32″N
SCA15	biotite-muscovite bearing granitoids	Sant'Andrea Apostolo dello Ionio/Serre p. unit	16°32′34.13″E	38°37′6.55″N
SCA24	biotite-muscovite bearing granitoids	Sant'Andrea Apostolo dello Ionio/Serre p. unit	16°32′34.11″E	38°36′20.64″N
SCA46	biotite-muscovite bearing granitoids	Sant'Andrea Apostolo dello Ionio/Serre p. unit	16°30′44.10″E	38°33′14.98″N
SCA47	biotite-muscovite bearing granitoids	Sant'Andrea Apostolo dello Ionio/Serre p. unit	16°30′13.57″E	38°33′9.19″N
SCA49	biotite-muscovite bearing granitoids	Sant'Andrea Apostolo dello Ionio/Serre p. unit	16°30′3.89″E	38°32′55.70″N
SCA51	biotite-muscovite bearing granitoids	Sant'Andrea Apostolo dello Ionio/Serre p. unit	16°30′5.73″E	38°33′1.49″N

Preprints.org (www.preprints.org) | NOT PEER-REVIEWED | Posted: 2 May 2026 doi:10.20944/preprints202604.2200.v1

SCA56	biotite-muscovite bearing granitoids	Sant'Andrea Apostolo dello Ionio/Serre p. unit	16°31′0.54″E	38°34′02″N
ccar67	biotite-muscovite bearing granitoids	Sant'Andrea Apostolo dello Ionio/Serre p. unit	16°32′19.39″E	38°37′20.10″N
SCA27	K-feldspar megacrysts granitoids	Isca sullo Ionio p. unit	16°29′25.74″E	38°40′24.11″N
SCA28	K-feldspar megacrysts granitoids	Isca sullo Ionio p. unit	16°29′25.74″E	38°40′24.11″N
SCA30	K-feldspar megacrysts granitoids	Isca sullo Ionio p. unit	16°29′25.74″E	38°40′24.11″N
SCA31	K-feldspar megacrysts granitoids	Isca sullo Ionio p. unit	16°29′25.74″E	38°40′24.11″N
SCA94	K-feldspar megacrysts granitoids	Sant'Andrea Apostolo dello Ionio/Serre p. unit	16°32′51.89″E	38°35′28.72″N
SCA95	K-feldspar megacrysts granitoids	Sant'Andrea Apostolo dello Ionio/Serre p. unit	16°32′41.4″E	38°35′21″N
SCA96	K-feldspar megacrysts granitoids	Sant'Andrea Apostolo dello Ionio/Serre p. unit	16°32′51.89″E	38°35′28.72″N
SCA97	K-feldspar megacrysts granitoids	Sant'Andrea Apostolo dello Ionio/Serre p. unit	16°32′44.4″E	38°35′22″N
SCA98	K-feldspar megacrysts granitoids	Sant'Andrea Apostolo dello Ionio/Serre p. unit	16°32′49.4″E	38°35′23″N
SCA99	K-feldspar megacrysts granitoids	Sant'Andrea Apostolo dello Ionio/Serre p. unit	16°32′51.89″E	38°35′28.72″N
SCA100	K-feldspar megacrysts granitoids	Sant'Andrea Apostolo dello Ionio/Serre p. unit	16°32′51.89″E	38°35′28.72″N
SCA101	K-feldspar megacrysts granitoids	Sant'Andrea Apostolo dello Ionio/Serre p. unit	16°32′51.89″E	38°35′28.72″N
SCA102	K-feldspar megacrysts granitoids	Sant'Andrea Apostolo dello Ionio/Serre p. unit	16°32′51.89″E	38°35′28.72″N
SCA104	K-feldspar megacrysts granitoids	Isca sullo Ionio p. unit	16°29′28.4″E	38°40′24″N
SCA105	K-feldspar megacrysts granitoids	Isca sullo Ionio p. unit	16°29′28.4″E	38°40′24″N
GO66	peraluminous microgranites	Cittanova p. unit	16° 7′11.60″E	38°20′19.79″N
GO67	peraluminous microgranites	Cittanova p. unit	16° 7′18.47″E	38°20′27.23″N
GO68	peraluminous microgranites	Cittanova p. unit	16° 5′21.03″E	38°20′46.61″N
GO69	peraluminous microgranites	Cittanova p. unit	16° 5′28.94″E	38°20′43.56″N
GO70	peraluminous microgranites	Cittanova p. unit	16° 5′28.94″E	38°20′43.56″N
SCA50	peraluminous microgranites	Sant'Andrea Apostolo dello Ionio/Serre p. unit	16°30′4.61″E	38°32′58.77″N

 doi:10.20944/preprints202604.2200.v1

SCA71	peraluminous microgranites	Sant'Andrea Apostolo dello Ionio/Serre p. unit	16°28'53.64"E	38°32'15.77"N
SCA73	peraluminous microgranites	Sant'Andrea Apostolo dello Ionio/Serre p. unit	16°28'52.98"E	38°32'20.76"N
SCA62	peraluminous microgranites	Sant'Andrea Apostolo dello Ionio/Serre p. unit	16°30'56.93"E	38°32'4.70"N
SCA5a	hypabyssal rocks	Sant'Andrea Apostolo dello Ionio/Serre p. unit	16°30'37.76"E	38°32'35.52"N
SCA6	hypabyssal rocks	Sant'Andrea Apostolo dello Ionio/Serre p. unit	16°30'40.43"E	38°32'35.81"N
SCA60	hypabyssal rocks	Sant'Andrea Apostolo dello Ionio/Serre p. unit	16°30'30.45"E	38°32'30.72"N
SCA63	hypabyssal rocks	Sant'Andrea Apostolo dello Ionio/Serre p. unit	16°29'48.21"E	38°32'6.25"N

Whole-rock chemical analyses, which constitute the dataset of the present paper, is available in the Database S1 as a Excel file, i.e., *Geochemistry_Samples_Serre.xlsx*.

The petrographic and structural characteristics of the granitoids are described below.

Concordant and discordant leucosomes are scattered within the deep crustal migmatitic rocks. Their composition ranges from leuco-tonalite to granite, depending on the host rocks and the presence of xenocrysts such as sillimanite, biotite, garnet and/or orthopyroxene. The melt composition is reflected by quartz, plagioclase, K-feldspar, biotite, and muscovite [15,32].

Coarse-grained granodiorites are characterized by large biotite clusters. They contain quartz, plagioclase, K-feldspar, and biotite; the granodioritic varieties exhibit higher proportion of plagioclase and resorbed actinolite-hornblende. Frequently, these rocks host microgranular mafic enclaves containing Mg-hornblende. They show a calc-alkaline and meta-luminous character [14].

Medium-grained muscovite granitoids exhibit a calc-alkaline, peraluminous character, as indicated by the presence of muscovite alongside quartz, K-feldspar, plagioclase, and biotite [9,14].

K-feldspar megacryst granitoids are characterized by large orthoclase crystals, measuring up to 5-6 cm, which are occasionally mantled by oligoclase-plagioclase. Their composition varies from granodiorite to granites; locally, they are calc-alkaline and may contain muscovite and rare microgranular biotite-bearing enclaves [7,8].

Peraluminous fine-grained granites display a fine-grained texture with a pervasive presence of muscovite and metamorphic xenoliths. They frequently contain cordierite, andalusite, garnet, and fibrolite dispersed in a matrix consisting of quartz, K-feldspar, and plagioclase [4,13,14].

Hypabyssal rocks in Permian dikes show porphyritic textures, with phenocrysts of amphibole, biotite, quartz, plagioclase, and K-feldspar. Their composition ranges from andesite to dacite.

3. Methods

Chemical analyses of granitoid samples were performed using X-ray fluorescence (XRF), except for Fe^{2+} and LOI. Samples were first reduced to powder in a planetary grinder equipped with agate jars and subsequently prepared as pressed pellets using polyvinyl alcohol as a binder.

Major and trace element concentrations in whole-rock samples were determined using a Philips PW1480/10 automatic spectrometer. For major elements, a Cr anti-cathode tube operating at 50 kV and 30 mA was used. Trace elements Ni, Cr, V, Ce, La, and Ba were detected using a W anti-cathode

 doi:10.20944/preprints202604.2200.v1

tube powered at 60kV and 45mA, while Rb, Sr, Y, Zr, and Nb were analyzed with a Rh anti-cathode tube operating at 60 kW and 45 mA. Fluorescence intensities were converted into oxides weight percentages of or trace elements concentrations (ppm) using a computational program based on the matrix effect correction method proposed by [37,38]. Two reference standards (AGV-1 of USGS-U.S.A. and NIM-G of NIM-South Africa) were used: precision is better than 5% for all elements, except for Ce, La and, Ba, for it is better than 10%.

Rare earth elements (REE) were measured at the CRPG laboratory in Nancy (France) using a Jobin Yvon™ JY70 inductively coupled plasma mass spectrometry (ICP-MS). For the BR standard, the laboratory reports a relative standard deviation (RDS) of less than 6% for all REE excluding Lu, based on 25 repeated analyses; for Lu, an RSD of 16% is reported.

FeO contents (where available) was measured volumetrically by titration with N/10 $KMnO_4$.

Loss of Ignition (LOI) was determined by calcination in a furnace at 900 °C.; the obtained values were subsequently corrected to occount for the oxidation of FeO to Fe_2O_3.

For a subset of samples, major and trace elements were determined by lithium metaborate/tetraborate fusion followed by ICP-MS at Actlabs laboratory (Canada).

Supplementary Materials: The following supporting information can be downloaded at: https://www.mdpi.com/article/doi/s1–to be attributed by the Journal, Geographic Data S1: file *Samples_Serre.kmz* for visualization in Google Earth of the sampling locations in the Serre Massif; Database S1: file *Geochemistry_Samples_Serre.xlsx* including whole-rock chemical analyses of the sample from the Serre Massif.

Author Contributions: Conceptualization, V.F.; methodology, A.F.; validation, A.F., F.M. and F.T.; data curation, A.F., F.M. and F.T.; writing—original draft preparation, review and editing, A.F., F.M., F.T. and V.F. All authors have read and agreed to the published version of the manuscript.

Funding: This research received no external funding.

Conflicts of Interest: The authors declare no conflicts of interest.

References

1. Winter, J.D. *Igneous Petrology*; Pearson: Upper Saddle River, NJ, USA, 2010.
2. De Vivo, B.; Ayuso, R. A.; Belkin, H. E.; Lima, A.; Messina, A.; Russo, S.; Viscardi, A. Whole-rock geochemistry and fluid inclusions as exploration tools for mineral deposits assessment in the Serre batholith, Calabria, southern Italy. *Eur. J. Miner.* **1992**, 4, 1035–1051.
3. Moresi, M.; Paglionico, A. Osservazioni geologiche, petrografiche e geochimiche sulle rocce granitoidi delle Serre orientali (Calabria). *Boll. Soc. Geol. It.* **1976**, 95(6), 1855–1882.
4. Crisci, G. M.; Maccarrone, E.; Rottura, A. Cittanova peraluminous granites (Calabria, Southern Italy). *Miner. Petrogr. Acta* **1979**, 23, 279–302.
5. Crisci, G.M., Paglionico, A. & Rottura,A. (1985). Tonalites from the Serre, CalabrianArc, southern Italy. Geological, petrological andgeochemical features. *Neues Jahrb. Mineral. Abh.* **1985**, 153(1), 59–75.
6. Del Moro, A.; Paglionico, A.; Piccarreta, G.; Rottura, A. Tectonic structure and evolution of the Serre, Calabrian Arc, southern Italy: geological, petrological and radiometric evidence. *Tectonophysics* **1986**, 124, 223-238.
7. Del Moro, A.; Fornelli, A.; Paglionico, A. K-feldspar megacryst granitic suite in the Serre (Southern Calabria - Italy). *Period. Mineral.* **1994**, 63, 19–33.
8. Rottura, A.; Bargossi, G.M.; Caironi, V.; Del Moro, A.; Maccarrone, E.; Macera, P.; Paglionico, A.; Petrini, R.; Piccarreta, G. Petrology, geochemistry and Sr, Nd isotopes of contrasting Hercynian granitoids from southern Calabrian Arc (southern Italy). *Miner. Petrogr. Acta* **1989**, 23, 1–36.
9. Rottura, A.; Bargossi, G.M.; Caironi, V.; Del Moro, A.; Maccarrone, E.; Macera, P.; Paglionico, A.; Petrini, R.; Piccarreta, G.; Poli, G. Petrogenesis of contrasting Hercynian granitoids from the Calabrian Arc, southern Italy. *Lithos* **1990**, 24(2), 97–119.
10. Rottura, A.; Caggianelli, A.; Campana, R.; Del Moro, A. Petrogenesis of Hercynian peraluminous granites from the Calabrian Arc, Italy. *Eur. J. Mineral.* **1993**, 5, 737–754.

11. Caggianelli, A.; Del Moro, A.; Paglionico, A.; Piccarreta, G.; Rottura, A. Lower crust granite genesis connected with chemical fractionation in the continental crust of Calabria (Southern Italy). *Eur. J. Miner.* **1991**, 3, 159–180.
12. Fornelli, A. Structure and genesis of potassium feldspar megacrysts in the Satriano granitoids, eastern Serre, Calabria. *Miner Petrogr. Acta* **1991**, 34, pp. 95–103.
13. Fornelli, A. Metamorphic xenoliths and microgranular enclaves in the Serre granodiorites (Southern Calabria-Italy): Their connection with granitoid genesis. *Mineral. Petrol.* **1994**, 51(1), 49–65.
14. Fornelli, A.; Caggianelli, A.; Del Moro, A.; Bargossi, G.M.; Paglionico, A.; Piccarreta G.; Rottura A. Petrology and evolution of the central Serre granitoids (Southern Calabria-Italy). *Period. Mineral.* **1994**, 63 (1-3), 53-70.
15. Fornelli, A.; Piccarreta, G.; Del Moro A.; Acquafredda, P. Multi-stage Melting in the Lower Crust of the Serre (Southern Italy). *J. Petrol.* **2002**, 43(12), 2191–2217.
16. Fornelli, A.; Piccarreta, G.; Acquafredda, P.; Micheletti, F.; Paglionico, A. Geochemical fractionation in migmatitic rocks from Serre Granulitic terrane (Calabria, southern Italy). *Period. Mineral.* **2004**, 73, 145-157.
17. Acquafredda P.; Fornelli A.; Micheletti F.; Piccarreta G. The abundance of 51 elements and petrovolumetric models of the Calabria crust: Curinga-Stilo area (site 6). In *Scritti e Documenti*; Accademia Nazionale delle Scienze detta dei XL: Roma, Italy 2003; pp. 263–288.
18. Romano, V.; Cirrincione, R.; Fiannacca, P.; Lustrino, M.; Tranchina, A. Late-Hercynian post-collisional dyke magmatism in central Calabria (Serre Massif, southern Italy). *Period. Mineral.* **2011**, 80(3), 489–515.
19. Fiannacca, P.; Cirrincione, R.; Bonanno, F.; Carciotto, M.M. Source-inherited compositional diversity in granite batholiths: The geochemical message of Late Paleozoic intrusive magmatism in central Calabria (southern Italy). *Lithos* **2015**, 236-237, 123–140.
20. Fiannacca, P.; Lombardo, R.; Militello, G.M.; Cirrincione, R. Plagioclase microstructures and compositions as tracers of mixing processes inweakly to strongly peraluminous granodiorites and granites from the Serre Batholith (southern Italy). *Rend. Online Soc. Geol. Ital.* **2016**, 38, 43–46.
21. Fiannacca, P.; Williams, I.S.; Cirrincione, R. Timescales and mechanisms of batholith construction: Constraints from zircon oxygen isotopes and geochronology of the late Variscan Serre Batholith (Calabria, southern Italy). *Lithos* **2017**, 277, 302–314.
22. Fiannacca, P.; Williams, I.S.; Cirrincione, R.; Pezzino, A. Poly-orogenic melting of metasedimentary crust from a granite geochemistry and inherited zircon perspective (southern Calabria-Peloritani orogen, Italy). *Front. Earth Sci.* **2019**, 7, 119.
23. Fiannacca, P.; Basei, M.A.; Cirrincione, R.; Pezzino, A.; Russo, D. Water-assisted production of late-orogenic trondhjemites at magmatic and subsolidus conditions. *Geol. Soc. Lond. Spec. Publ.* **2020**, 491(1), 147–178.
24. Biget, T.; Bruand, E.: Langone, A.; Boyet, M.; Caggianelli, A.; Bonnand, P. Tracing anatexis and bottom-up crustal homogenisation with in situ Sm-Nd isotopes. *Geochem. Perspect. Lett.* **2026**, 38, 46–52.
25. Appelo, C.A.J.; Postma, D. *Geochemistry, Groundwater and Pollution*; Balkema: Rotterdam, The Netherlands, 2005.
26. Festa, V.; Messina, A.; Paglionico, A.; Piccarreta, G.; Rottura, A. Pre-Triassic history recorded in the Calabria–Peloritani segment of the Alpine chain, southern Italy. An overview. *Period. Mineral*. **2004**, 73, 57–71.
27. Festa, V.; Di Battista, P.; Caggianelli, A.; Liotta, D.. Exhumation and tilting of the late-Hercynian continental crust in the Serre Massif (Southern Calabria, Italy). *Boll. Soc. Geol. It.* **2003**, Volume Speciale 2, 79–88.
28. Caggianelli, A.; Prosser, G.; Rottura, A. Thermal history vs. fabric anisotropy in granitoids emplaced at different crustal levels: An example from Calabria, Southern Italy. *Terra Nova* **2000**, 12, 109–116.
29. Langone, A.; Caggianelli, A.; Festa, V.; Prosser, G. Time constraints on the building of the Serre Batholith: Consequences for the thermal evolution of the Hercynian continental crust exposed in Calabria (southern Italy). *J. Geol.* **2014**, 122, 183–199.
30. Servizio Geologico d'Italia. *Carta Geologica d'Italia alla scala 1:50.000, F. 580 Soverato*; ISPRA.: Roma, Italy, 2015.
31. Servizio Geologico d'Italia. *Carta Geologica d'Italia alla scala 1:50.000, F. 590 Taurianova*; ISPRA: Roma, Italy, 2017.

 doi:10.20944/preprints202604.2200.v1

32. Del Moro, A.; Fornelli, A.; Piccarreta, G. Disequilibrium melting in granulite facies metasedimentary source of the northern Serre (Calabria–Southern Italy). *Mineral. Petrol.* **2000**, 70, 89–104.
33. Festa, V.; Caggianelli, A.; Langone, A.; Prosser, G. Time–space relationships among structural and metamorphic aureoles related to granite emplacement: A case study from the Serre Massif (southern Italy). *Geol. Mag.* **2013**, 150, 441–454.
34. Tursi, F.; Spiess, R.; Festa, V.; Fregola, R.A. Hercynian subduction-related processes within the metamorphic continental crust in Calabria (southern Italy). *J. Metamorph. Geol.* **2020**, 38, 771–793.
35. Fornelli, A.; Festa, V.; Micheletti, F.; Spiess, R.; Tursi, F. Building an orogen: Review of U-Pb zircon ages from the Calabria–Peloritani terrane to constrain the timing of the southern Variscan belt. *Minerals* **2020**, 10, 944.
36. Fregola, R.A.; Ciccolella, A.; Festa, V.; Ruggieri, G.; Schingaro, E.; Tursi, F.; Ventruti, G. Review of Polymetallic Mineralization in the Sila and Serre Massifs (Calabria, Southern Italy). *Minerals* **2023**, 13(3), 439.
37. Leoni, L.; Saitta, M. X-ray fluorescence analysis of 29 trace elements in rock and mineral standards. *Rend. Soc. Ital. Mineral. Petrol.* **1976**, 32(2), 497–510.
38. Leoni, L.; Saitta, M. Determination of yttrium and niobium on standard silicate rocks by X-ray fluorescence analyses. *X-Ray Spectrom.* **1976**, 5, 29–30.